

Long-term Baseline Ozone Changes in the Western US: A Synthesis of Analyses

David D. Parrish¹, Richard G. Derwent², and Ian C. Faloona³

¹David.D.Parrish, LLC

²rdscientific

³University of California, Davis

November 24, 2022

Abstract

Quantification of the magnitude and long-term changes of ozone concentrations transported into the US is important for effective air quality policy development. We synthesize multiple published trend analyses of western US baseline ozone, and show that all results are consistent with an overall, non-linear change – rapid increase during the 1980s that slowed in the 1990s, maximized in the mid-2000s, and was followed by a slow decrease thereafter. This non-linear change accounts for $\sim 2/3$ of the variance in the published linear trend analyses; we attribute the other $1/3$ to unquantified autocorrelation in the analyzed data sets. Recent systematic changes in baseline ozone at the US West Coast have been relatively small - the standard deviation of the 2-year means over the 1990-2017 period is 1.5 ppb. International efforts to reduce anthropogenic precursor emissions from all northern mid-latitude sources could possibly reduce baseline ozone concentrations, thereby improving US ozone air quality.

1 **Long-term Baseline Ozone Changes in the Western US:**
2 **A Synthesis of Analyses**

3
4 **David D. Parrish^{1,2}, Richard G Derwent³, and Ian C. Faloona^{2,4}**

5 ¹ David.D.Parrish, LLC, Boulder, Colorado, USA

6 ² Air Quality Research Center, University of California, Davis, California USA

7 ³ rdsscientific, Newbury, Berkshire, UK

8 ⁴ Department of Land, Air, & Water Resources, University of California, Davis, California, USA

9
10 Corresponding author: David D. Parrish, (david.d.parrish.llc@gmail.com)

11
12 **Key Points:**

- 13 • Reported trends in tropospheric ozone concentrations transported into the Western US
14 vary between -2.8 to +7.0 ppb/decade
- 15 • All reported trends agree with an overall non-linear change – ozone increasing before the
16 mid-2000s and slowly decreasing thereafter
- 17 • About 1/3 of the variance in reported trends is due to autocorrelation in the data, which
18 was not adequately considered in prior analyses
- 19

20 **Abstract**

21 Quantification of the magnitude and long-term changes of ozone concentrations
22 transported into the US is important for effective air quality policy development. We synthesize
23 multiple published trend analyses of western US baseline ozone, and show that all results are
24 consistent with an overall, non-linear change – rapid increase during the 1980s that slowed in the
25 1990s, maximized in the mid-2000s, and was followed by a slow decrease thereafter. This non-
26 linear change accounts for $\sim 2/3$ of the variance in the published linear trend analyses; we
27 attribute the other $1/3$ to unquantified autocorrelation in the analyzed data sets. Recent systematic
28 changes in baseline ozone at the US West Coast have been relatively small - the standard
29 deviation of the 2-year means over the 1990-2017 period is 1.5 ppb. International efforts to
30 reduce anthropogenic precursor emissions from all northern mid-latitude sources could possibly
31 reduce baseline ozone concentrations, thereby improving US ozone air quality.

32

33 **Plain Language Summary**

34 Ozone is an air pollutant with significant human and ecological health impacts. Air masses
35 transported into the western US from over the Pacific Ocean carry ozone concentrations that are,
36 on average, a large fraction of the US health standard, so quantifying these trans-boundary
37 concentrations are important for developing a complete picture of US air quality. Published
38 analyses of temporal trends of these transported ozone concentrations vary widely, from early
39 reports of increases to more recent reports of decreases. We show that the long-term ozone
40 changes have been nonlinear, with concentration increases before the mid-2000s, followed by
41 decreases thereafter. Superimposed on the overall changes is significant interannual variability
42 that makes accurate determination of systematic trends over decade-scale time periods uncertain.
43 The recent decreases in transported ozone concentrations is good news for US air quality, as it
44 eases the difficulty of achieving the ozone air quality standard.

45 **1 Introduction**

46 Air masses from the Pacific marine environment enter the continental atmosphere over
47 the western US carrying ozone concentrations determined by natural and anthropogenic sources
48 and sinks in upwind regions. These transported ozone concentrations are large enough to
49 significantly impact air quality in urban and rural US locations; fully understanding this impact
50 requires characterization of the temporal and spatial distribution of those ozone concentrations.
51 Over the past two decades, a number of observational-based studies have quantified the average
52 ozone concentration changes at specific western US locations thought to represent changes in the
53 transported marine air; Table 1 lists 28 of these quantifications. Reported average trends over
54 different time periods vary widely, from relatively large increases to smaller magnitude
55 decreases. Our goal in this study is to synthesize these disparate results, and to develop a
56 consistent picture of the overall, decadal-scale temporal change in the transported ozone
57 concentrations over the past 3 to 4 decades at the US west coast.

58 A conceptual picture provides a useful framework for understanding the temporal
59 variation of ozone at northern mid-latitudes. On average, prevailing westerly winds define a
60 circulating air stream repeatedly passing over all continents and oceans. The average net lifetime
61 of ozone at these latitudes (~ 100 days) is longer than the circum-global transport time (~ 30
62 days). Overall, the long lifetime and zonal transport imply that a mean ozone concentration is

63 established on a time scale of weeks to months, and that this mean concentration is similar
64 throughout northern mid-latitudes; we roughly estimate that this similarity is within $\pm 10\%$ from
65 the top of the planetary boundary layer to ~ 9 km at all longitudes (e.g., see Figure 5 of Parrish et
66 al., 2020). This picture also implies a relatively smooth and systematic seasonal cycle of ozone in
67 baseline air masses. A zonally similar mean does not imply a lack of ozone variability, as ozone
68 varies about that mean on a wide spectrum of shorter and longer time scales, including decadal
69 climate variability (e.g., Lin et al., 2014), sporadic events such as wildfires (Lin et al., 2017), and
70 heatwaves and droughts (Lin et al., 2020). The first four sections of the Supporting Information
71 describe this conceptual picture and ozone variability in more detail.

72 The subject of this study is decadal and longer scale ozone changes, which are caused by
73 long-term changes in precursor emissions and the changing climate; quantifying these changes
74 must account for the variability of ozone on the wide spectrum of shorter time scales, variability
75 that tends to obscure the long-term changes of interest. Importantly, our guiding conceptual
76 picture implies that these long-term changes must be zonally similar, since it is the zonally
77 similar average ozone concentration that must change; a recent analysis of baseline ozone
78 concentrations at the west coasts of North America and Europe (Parrish et al., 2020) document
79 this expected zonal similarity.

80 Several terms appear in the literature in reference to the transported ozone concentrations.
81 A common general term is background ozone. However, it is important to note that presently
82 observed concentrations do not represent natural ozone concentrations, i.e., those that existed
83 before industrial development, since anthropogenic emissions of ozone precursors have
84 increased ozone concentrations throughout northern mid-latitudes. For clarity, in this work we
85 adopt the term “baseline” (e.g., see discussion in Chapter 1 of HTAP, 2010) to refer to ozone
86 concentrations measured at western US locations that receive transported marine air without
87 significant perturbation from recent local or regional North American influences. It is the long-
88 term change in these baseline concentrations that we seek to quantify.

89 In addition to the linear trend analyses included in Table 1, two published analyses
90 utilized non-linear approaches to quantify long-term changes of baseline ozone concentrations at
91 northern mid-latitudes; both reached similar conclusions. Logan et al. (2012) analyzed several
92 European baseline ozone data sets that extended through 2009, and showed that ozone increased
93 by 6.5-10 ppb in 1978-1989 and 2.5-4.5 ppb in the 1990s, with that increase ending and a
94 maximum reached in the 2000s, followed by decreasing concentrations, at least in summer.
95 Parrish et al. (2020) analyzed those same data sets, which by then extended through 2018, plus
96 additional European and North American data sets; in total 8 baseline data sets from surface
97 sites, balloon-borne sondes and aircraft over western Europe and western North America were
98 considered. These measurements covered altitudes from sea level to 9 km. Again, an initial,
99 relatively rapid increase was observed, with ozone concentrations reaching a maximum in the
100 mid-2000s, followed by decreasing concentrations. An important conclusion of these analyses is
101 that, within statistical confidence limits, the same non-linear long-term baseline ozone change
102 has occurred throughout northern mid-latitudes at all altitudes. The goal of this paper is to
103 compare and contrast published linear trend and non-linear long-term change analyses of multi-
104 decadal ozone time series collected at the surface and in the free troposphere over the western
105 US, and to synthesize those analyses to provide an accurate and complete geophysical
106 quantification of long-term changes in baseline ozone at the US West Coast.

107 2 Materials and Methods

108 As discussed above, a relatively large number of analyses of long-term baseline ozone
 109 changes have been published based upon ozone time series collected in the continental western
 110 US. This work is based upon the results of those analyses; no new data sets are analyzed.

111 Any analysis aiming to quantify the overall long-term change in tropospheric ozone at
 112 northern mid-latitudes must effectively deal with two issues: the non-linearity of the long-term
 113 changes that have been documented in previous work, and the substantial interannual variability
 114 in mean ozone concentrations that tends to obscure the long-term changes. All linear trend
 115 analyses return a single parameter value that quantifies the trend; this is effectively an average
 116 slope of the long-term change over the span of the analyzed time series. Hence, by its very nature
 117 linear trend analysis is ill-suited to quantify non-linear, long-term changes.

118 Without a priori knowledge of the functional form of the ozone concentration changes,
 119 long-term change analysis is generally based either on linear trend analyses or on fits of the first
 120 few terms of a power series to measured ozone concentrations. A power series fit does not
 121 assume any particular functional form for the time evolution; it is quite flexible, as it provides a
 122 quantitative description of the average continuous, long-term change in any series of
 123 observations (Parrish et al., 2019). The power series fit is obtained through a regression fit of a
 124 polynomial to the measurements, with retention of only the statistically significant terms to avoid
 125 over fitting the time series. In this work no more than the first three terms are considered,

$$126 \quad \text{O}_3 = a + bt + ct^2, \quad (1)$$

127 because no more than three statistically significant terms (i.e., those with 95% confidence
 128 intervals not containing zero) are encountered in any fits in this study. Fits with only the first two
 129 terms statistically significant are equivalent to linear regressions. A statistically significant third
 130 term indicates the average long-term change is non-linear, i.e. $d^2\text{O}_3/dt^2$ is non-zero, but it does
 131 not indicate that the overall change is necessarily parabolic. Equation 1 does not account for
 132 seasonal variations; these variations are eliminated by fitting to annual means, seasonal means,
 133 or deseasonalized monthly means (sometimes called monthly residuals or monthly anomalies).
 134 Ozone concentrations are consistently quantified as mixing ratios, with units of 10^{-9} mole O_3 per
 135 mole air, denoted as ppb.

136 The time origin is chosen as the year 2000 (i.e., t in Equation 1 equals the year - 2000) to
 137 ensure precise determination of the coefficients in Equation 1. The first coefficient (a , with units
 138 ppb O_3) is then the intercept of the fitted curve at the year 2000, and quantifies the absolute
 139 concentration at that year. The second coefficient (b , with units ppb O_3 year⁻¹) is the slope of the
 140 fitted curve at that year, and gives the best estimate of the time rate of change of O_3 in 2000. The
 141 third coefficient (c , with units ppb O_3 year⁻²) gives the constant curvature of the fit. For non-
 142 linear fits, a negative value is generally derived for c ; such curves indicate ozone concentrations
 143 increasing early in the data record, reaching a maximum, and then decreasing at later times. The
 144 year of that maximum is

$$145 \quad \text{year}_{\text{max}} = 2000 - b/2c. \quad (2)$$

146 Parameter values taken from published analyses are generally given with specified 95%
 147 confidence limits. We also specify 95% confidence limits in this work. However, it is important
 148 to recognize that confidence limits reported in the literature are generally derived from the
 149 variability of the data points about the fitted line or curve without a full analysis of the

150 autocorrelation in those data. As a consequence, the quoted confidence limits are generally
151 underestimated to an unknown extent. This issue is important to the present discussion, when
152 comparing and contrasting results from different analyses.

153 Within the baseline troposphere, average ozone concentrations do exhibit some
154 systematic spatial variability, despite the general zonal uniformity at northern mid-latitudes; in
155 particular baseline ozone concentrations generally increase with altitude (e.g., Oltmans et al.,
156 2008). To remove this systematic variability when comparing long-term changes derived from
157 data sets with different mean concentrations, fits of Equation 1 are normalized to zero at the year
158 2000 by subtracting the corresponding values of the a parameter. The normalization of a linear
159 fit to a quadratic fit is discussed in the following section.

160 Polynomial fits have been used previously to quantify long-term changes in ozone
161 concentrations (e.g., Logan et al., 2012; Parrish et al., 2012; 2017; 2020; Derwent et al., 2018).
162 Such fits, as well as linear fits, are not based on a physical model of the observed temporal
163 changes, so they cannot be reliably extrapolated to times outside the period of observations. For
164 ease of presentation and discussion, the values of the b and c parameters are given as ppb O₃
165 decade⁻¹ and ppb O₃ decade⁻², respectively. The Section S5 of the Supporting Information
166 discusses the relation of polynomial fits and linear trend analysis in more detail, including their
167 respective advantages and disadvantages.

168 **3 Results and Discussion**

169 The results of Parrish et al. (2020) are reproduced in Figure 1a: deseasonalized,
170 normalized monthly means from each of eight data sets considered (gray points), 2-year averages
171 of those monthly means (black symbols with error bars indicating standard deviations), and a
172 quantification of the average long-term baseline ozone change (black curve). This curve is the
173 least-squares fit of a quadratic polynomial (i.e., Equation 1) to the monthly means. Table 2 gives
174 the parameters of the fit; Equation 2 indicates that a maximum average baseline ozone
175 concentration was reached in the year 2005.7 ± 2.5 . Figure 1a also includes quadratic polynomial
176 fits to time series from a US Pacific marine boundary layer (MBL) data set and from one higher
177 altitude (1.8 km) site further inland operated by the National Park Service at Lassen Volcanic
178 National Park. Parrish et al. (2017) analyzed these data sets to demonstrate that the long-term
179 trend in baseline ozone concentrations at the US West Coast had reversed from an early increase
180 to a later decrease, with a maximum reached in early to mid-2000s; Figure 1a extends the
181 analysis of those data sets through 2017. These are also two of the eight data sets analyzed by
182 Parrish et al. (2020). There are apparent differences between the three curves, most prominently
183 a more rapid recent decrease in the Pacific MBL data; however, Table 2 shows that the
184 parameters from both the Lassen Volcanic NP and the Pacific MBL fits agree with those of the
185 northern mid-latitude quadratic fit of Parrish et al. (2020) within their indicated confidence
186 limits. Thus, there is no statistically significant difference between the three quadratic fits.

187 Previously published linear trend analyses of ozone changes within the western US are
188 compared with the results of Parrish et al. (2020) in Figure 1b and Table 1 includes reported
189 trends from 28 separate analyses. A selected sample of those trend results are represented by
190 straight line segments with slopes equal to the reported trends and with lengths equal to the time
191 spans of the analyzed data sets. Each straight line segment is normalized to the non-linear
192 analysis results by minimizing the sum of the square of the deviations between the line segment
193 and the 2-year averages (black symbols in Figure 1b) that fall within the time span of the

194 corresponding data set. A common general feature characterizes these results – the earlier the
 195 start and end times of the trend analysis, the larger the quantified trend. This feature follows from
 196 the slowing of the increase in baseline ozone indicated by the black curve in Figure 1. The three
 197 earlier analyses (Jaffe et al., 2003; Parrish et al., 2009; and Cooper et al., 2010) consider data
 198 predominately from before the baseline ozone maximum was reached, and therefore report the
 199 larger trends. The multiple analyses of Cooper et al. (2020) and the two analyses of Gaudel et al.
 200 (2020) cover later time periods that include the ozone maximum with extended periods on either
 201 side; they therefore report small trends, some positive and some negative. Cooper et al. (2020)
 202 report three analyses, with progressively later starting times for each of 4 data sets; the derived
 203 trends become progressively more negative for the later starting times. These features of the
 204 linear trend analyses are all consistent with the overall behavior of the quadratic analysis
 205 indicated by the black curve.

206 The 28 referenced trend analyses considered data sets covering a total of 34 years (1984-
 207 2017) and derived widely varying trends (-2.8 to +7.0 ppb/decade). The nonlinearity of the long-
 208 term change accounts for much of these differences, but interannual variability about that long-
 209 term change also contributes to differences in the results. The analysis of Cooper et al. (2010)
 210 gave the largest trend (+7.0 ppb/decade); Lin et al. (2015) show that this result was an
 211 overestimate, as were 5 related analyses (Cooper et al., 2012; Lin et al., 2015), due to substantial
 212 influences from interannual variability. None of the 28 trend analyses accounts for uncertainties
 213 introduced into the results from the autocorrelation in data sets associated with interannual
 214 variability, although some address shorter-term, month-to-month autocorrelation (e.g., Gaudel et
 215 al., 2020). Section S6 of the Supporting Information discuss illustrates longer-term
 216 autocorrelation in two example data sets. The analysis based on the non-linear, least-squares fit
 217 included in Figure 1 (Parrish et al., 2020) effectively addresses both non-linearity and the longer-
 218 term autocorrelation in the longer, 40-year (1978-2017) data set. The resulting quadratic
 219 polynomial fit is derived from deseasonalized monthly means, but a fit to the 2-year averages of
 220 those monthly means gives nearly identical parameter values, but with significantly larger
 221 confidence limits; these larger confidence limits are included in Table 1. The high degree of
 222 temporal and spatial averaging in the 2-year means greatly reduces the influence of the
 223 autocorrelation associated with interannual variability.

224 We conclude that the black curve in Figure 1 provides a realistic and accurate
 225 quantification of the decadal-scale baseline ozone changes over the western US. The results of
 226 all published trend analyses are generally consistent with this non-linear fit over the shorter time
 227 periods of the trend analyses. The result of each linear trend analysis can be quantitatively
 228 compared with the average trend quantified by the quadratic curve over the time period of the
 229 trend analysis, which is equal to the slope of a straight line segment connecting the two points on
 230 the quadratic fit at the beginning (t_1) and end (t_2) times of the period included in the trend
 231 analysis:

$$232 \text{ slope} = b + c \cdot (t_1 + t_2). \quad (3)$$

233 Table 1 compares the slopes calculated from Equation 3 with the published trends, and Figure 2a
 234 shows their overall relationship. The quadratic fit accounts for ~67% of the variance in the 28
 235 linear trend analysis results. We attribute the remaining ~33% of the variance to the influence of
 236 interannual variability and to any spatial differences between trends at the measurement
 237 locations, which include surface sites in marine and continental environments, as well as data
 238 sets from the lower and mid free troposphere.

239 It is possible to independently determine a quadratic description of the overall long-term
240 ozone changes from the reported linear trends. Equation 3 indicates that a plot of the derived
241 trends as a function of the centers of the time periods of the respective trend determinations will
242 define a straight line with a slope of $2*c$ and a y-intercept of b of a quadratic curve as given by
243 Equation 1. Figure 2b shows that plot, which includes a linear regression to the 28 trend
244 determinations. Note that the x-intercept corresponds to the time that the trend is zero, i.e. the
245 year_{max} given by Equation 2. Table 2 compares the parameters from this quadratic determination
246 with the three discussed previously; generally there is agreement within the indicated confidence
247 limits, but reasons for exceptions to this agreement are discussed below.

248 The error bars illustrated in Figure 2a indicate the 95% confidence limits reported for the
249 respective trends. The fraction of these error bars not overlapping the 1:1 line (~50%) is much
250 larger than the expected 5%. (In Table 1 confidence limits are also included for the slopes
251 derived from the quadratic curve through a propagation of error calculation based on the
252 confidence limits of the quadratic parameters indicated in Table 2; inclusion of these confidence
253 limits does not significantly increase the number of points in Figure 2a that overlap the 1:1 line.)
254 Similarly, the parameter values compared in Table 1 do not agree in all cases within the derived
255 confidence limits. We attribute this disagreement primarily to underestimation of the confidence
256 limits derived in the trend analyses due to inadequate treatment of the autocorrelation in the data
257 sets resulting from interannual variability. The trends derived in the six earlier analyses of
258 springtime ozone mixing ratios in the free troposphere over western North America (Cooper et
259 al., 2010; 2012; Lin et al., 2015) all are particularly influenced by interannual variability, as
260 discussed by Lin et al. (2015). Increasing all confidence limits for the trends in Table 1 and the
261 lower three rows of Table 2 by 50% brings the fraction of the error bars in Figure 2 overlapping
262 the 1:1 line into close agreement with expectations, and eliminates the disagreements in Table 2.
263 The scatter of the trend analyses about the fits in Figure 2 emphasizes the importance of careful
264 consideration of the impact of autocorrelation in time series of ozone measurements caused by
265 interannual variability.

266 **4 Summary and Conclusions**

267 The long net lifetime of ozone in the prevailing westerly winds at northern mid-latitudes
268 implies that a common long-term change in mean baseline ozone concentrations must have
269 occurred throughout this zone. Parrish et al. (2020) document this similarity and quantify the
270 long-term change with a fit of a quadratic polynomial to monthly and biennial means of multiple
271 data sets. Linear trends reported for different time periods in 28 published analyses of western
272 US baseline ozone data sets vary between -2.8 to +7.0 ppb/decade. The quadratic fit of Parrish et
273 al. (2020) accounts for about two-thirds of the variance in the trend results, with the remaining
274 one-third attributed to interannual variability, which adds uncertainty to the trend determinations.
275 All reported trend analyses for western US baseline ozone data sets are consistent with the
276 picture conveyed by that quadratic fit - ozone increasing at the beginning of measurement
277 records with the rate of that increase progressively slowing, and ozone reaching a maximum in
278 the mid-2000s and decreasing thereafter. The quadratic fit provides an excellent fit to the twenty
279 2-year means over the 1978-2017 period, capturing about 89% of their variance with a root-
280 mean-square deviation between the fit and the means of 1.3 ppb; that fit also captures about 67%
281 of the variance in the 28 trend analyses, and agrees well with a quadratic fit derived from the
282 trend analysis results themselves.

283 Baseline ozone transported into the US constitutes a large fraction of the 70 ppb ozone
284 National Ambient Air Quality Standard (NAAQS); thus changes in baseline concentrations
285 affect the difficulty of achieving the NAAQS in US nonattainment areas. During the 1980s and
286 1990s those baseline concentrations were increasing, making attainment of US air quality goals
287 progressively more difficult and partially offsetting the air quality improvement that resulted
288 from emission controls (Jacob et al., 1999). In the mid-2000s baseline ozone concentrations
289 maximized and then slowly decreased at an average rate of 0.9 ± 0.8 ppb decade⁻¹ over the 2000-
290 2018 period (Parrish et al., 2020). This small decrease, if continued, would gradually lessen the
291 difficulty of achieving US air quality goals. However, despite the changes evident in Figure 1,
292 since 1990 average baseline ozone concentrations entering the western US exhibit little overall
293 change; the standard deviation of the fourteen 2-year means over the 1990-2017 period is only
294 1.5 ppb. Improvement in US ozone air quality has come primarily from continued precursor
295 emission controls that reduce local and regional photochemical ozone production; this
296 improvement can continue and possibly be augmented by international efforts to reduce
297 anthropogenic precursor emissions from all sources at northern mid-latitudes, thereby reducing
298 the hemisphere-wide transported baseline ozone concentrations.

299 **Acknowledgments, Samples, and Data**

300 The authors are grateful for the extensive ozone trend analyses that have been published
301 in the scientific literature; all analysis results on which this paper is based are reported in the
302 references included in Table 1 and Parrish et al. (2020). The Pacific MBL and Lassen Volcanic
303 NP data in Figure S3 are from Table S1 of Parrish et al. (2021) and the U.S.National Park
304 Service (<https://ardrequest.air-resource.com/data.aspx>, last accessed 18 February 2020),
305 respectively. This work was not supported by any funding agency, and the authors have
306 no conflicts of interests.

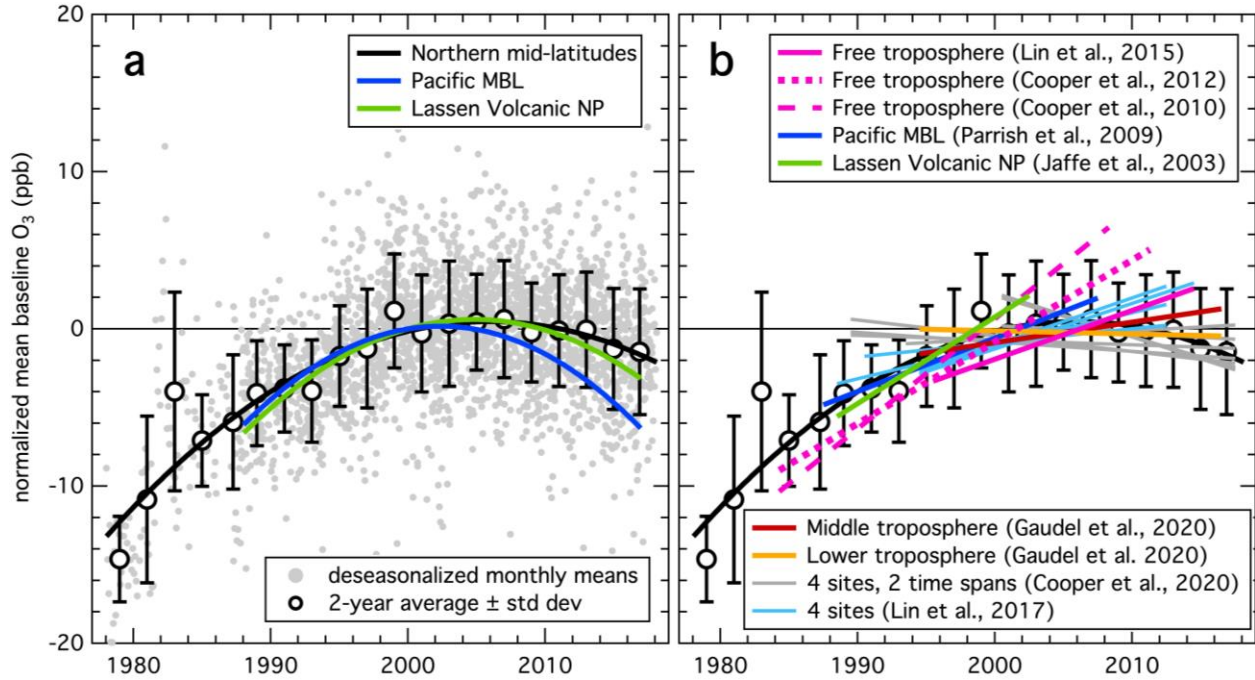
307 **References**

- 308 Cooper, O. R., et al. (2010). Increasing springtime ozone mixing ratios in the free troposphere
309 over western North America, *Nature*, 463(7279), 344–348, doi:10.1038/nature08708.
- 310 Cooper, O. R., Gao, R.-S., Tarasick, D., Leblanc, T. & Sweeney, C. (2012). Long-term ozone
311 trends at rural ozone monitoring sites across the United States, 1990–2010, *J. Geophys.*
312 *Res.*, 117, D22307, doi:10.1029/2012JD018261.
- 313 Cooper, O. R., et al. (2014). Global distribution and trends of tropospheric ozone: An
314 observation-based review. *Elem Sci Anth* 2: 29. DOI:
315 <https://doi.org/10.12952/journal.elementa.000029>
- 316 Cooper, O. R., et al. (2020). Multi-decadal surface ozone trends at globally distributed remote
317 locations, *Elem. Sci. Anth.*, 8, 23. doi.org/10.1525/elementa.420
- 318 Gaudel, A., et al. (2020). Aircraft observations since the 1990s reveal increases of tropospheric
319 ozone at multiple locations across the Northern Hemisphere, *Sci. Adv.*, 6, eaba8272.
- 320 HTAP (2010). Hemispheric transport of air pollution 2010, part A: Ozone and particulate matter,
321 air pollution studies no. 17, edited by: Dentener F., Keating T., & Akimoto H., United
322 Nations, New York and Geneva.

- 323 Jacob, D. J., Logan, J. A., & Murti, P. P. (1999). Effect of rising Asian emissions on surface
324 ozone in the United States, *Geophys. Res. Lett.*, *26*, 2175–2178,
325 doi:10.1029/1999GL900450.
- 326 Jaffe, D., Price, H., Parrish, D. D., Goldstein, A., & Harris, J. (2003). Increasing background
327 ozone during spring on the west coast of North America, *Geophysical Research Letters*,
328 *30*(12), 1613. doi.org/10.1029/2003GL017024
- 329 Lin, M., Horowitz, L. W., Oltmans, S. J., Fiore, A. M., & Fan, S. (2014). Tropospheric ozone
330 trends at Mauna Loa observatory tied to decadal climate variability. *Nature Geoscience*,
331 *7*(2), 136–143. <https://doi.org/10.1038/ngeo2066>
- 332 Lin, M., Horowitz, L. W., Cooper, O. R., Tarasick, D., Conley, S., Iraci, L. T., Johnson, B.,
333 Leblanc, T., Petropavlovskikh, I. & Yates, E. L. (2015). Revisiting the evidence of
334 increasing springtime ozone mixing ratios in the free troposphere over western North
335 America, *Geophys. Res. Lett.*, *42*, doi:10.1002/2015GL065311
- 336 Lin, M., Horowitz, L. W., Oltmans, S. J., Fiore, A. M. & Fan, S. (2017). US surface ozone trends
337 and extremes from 1980 to 2014: quantifying the roles of rising Asian emissions,
338 domestic controls, wildfires, and climate, *Atmos. Chem. Phys.*, *17*, 2943–2970.
- 339 Lin, M., Horowitz, L. W., Xie, Y., Paulot, F., Malyshev, S., Shevliakova, E., et al. (2020).
340 Vegetation feedbacks during drought exacerbate ozone air pollution extremes in Europe.
341 *Nature Climate Change*, *10*(5), 444–451. <https://doi.org/10.1038/s41558-020-0743-y>
- 342 Logan, J. A., Staehelin, J., Megretskaia, I. A., Cammas, J.-P., Thouret, V., Claude, H., et al.
343 (2012). Changes in ozone over Europe: Analysis of ozone measurements from sondes,
344 regular aircraft (MOZAIC) and alpine surface sites. *Journal of Geophysical Research*,
345 *117*, D09301. <https://doi.org/10.1029/2011JD016952>
- 346 Oltmans, S. J., Lefohn, A. S., Harris, J. M., & Shadwick, D. S. (2008), Background ozone levels
347 of air entering the west coast of the U.S. and assessment of longer-term changes, *Atmos.*
348 *Environ.*, *42*, 6020–6038, doi:10.1016/j.atmosenv.2008.03.034.
- 349 Parrish, D. D., Millet, D. B., & Goldstein, A. H. (2009). Increasing ozone in marine boundary
350 layer air inflow at the west coasts of North America and Europe, *Atmospheric Chemistry*
351 *and Physics*, *9*, 1303–1323.
- 352 Parrish, D. D., Law, K. S., Staehelin, J., Derwent, R., Cooper, O. R., Tanimoto, H., et al. (2012).
353 Long-term changes in lower tropospheric baseline ozone concentrations at northern mid-
354 latitudes. *Atmospheric Chemistry and Physics*, *12*, 11,485–11,504.
355 <https://doi.org/10.5194/acp-12-11485-2012>
- 356 Parrish, D. D., Petropavlovskikh, I., & Oltmans, S. J. (2017). Reversal of long-term trend in
357 baseline ozone concentrations at the North American West Coast. *Geophys. Res. Lett.*, *44*.
358 <https://doi.org/10.1002/2017GL074960>
- 359 Parrish, D. D., Derwent, R. G., O'Doherty, S. & Simmonds, P. G. (2019). Flexible approach for
360 quantifying average long-term changes and seasonal cycles of tropospheric trace species,
361 *Atmos. Meas. Tech.*, *12*, 3383–3394, <https://doi.org/10.5194/amt-12-3383-2019>

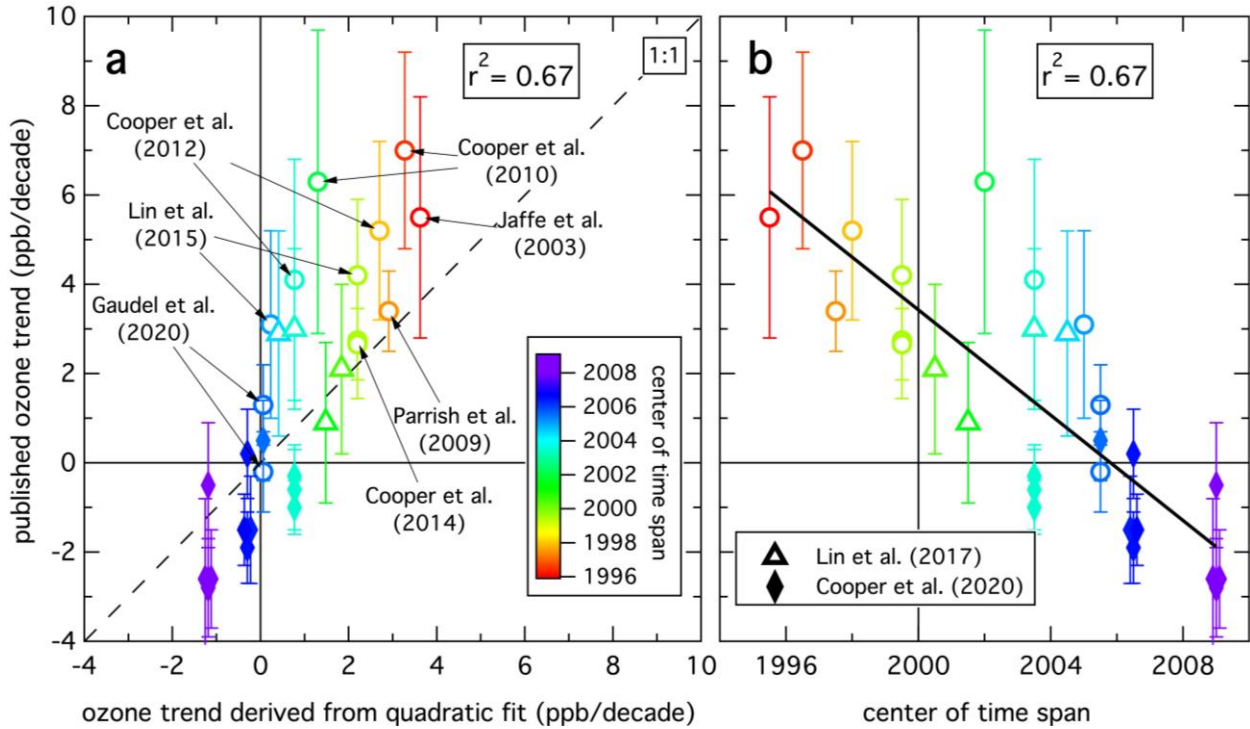
362 Parrish, D. D., et al. (2020), Zonal similarity of long-term changes and seasonal cycles of
363 baseline ozone at northern mid-latitudes. *J. Geophys. Res.: Atmos.*, doi:
364 10.1029/2019JD031908

365 Parrish, D. D., et al. (2021), Anthropogenic Reversal of the Natural Ozone Gradient between
366 Northern and Southern Mid-latitudes. *Atmos. Chem. Phys. Disc.*,
367 <https://doi.org/10.5194/acp-2020-1198>
368



369

370 **Figure 1.** Long-term changes in baseline ozone at northern mid-latitudes. **(a)** Normalized,
 371 deseasonalized monthly mean data (gray points) from eight baseline data sets collected at the
 372 surface and in the free troposphere in western North America and western Europe. The symbols
 373 with error bars are 2-year means with standard deviations of the gray points, the black solid
 374 curve is a quadratic polynomial fit to the gray points. The colored curves are quadratic fits from
 375 analyses of two western US data sets (Parrish et al., 2020). **(b)** Quadratic fit and 2-year means
 376 from **(a)** compared to line segments representing the annotated trend determinations from
 377 western US data sets covering varying time periods included in Table 1.



378

379 **Figure 2.** (a) Correlation between published ozone trends (Table 1) and those calculated for the
 380 same time periods from the long-term northern mid-latitude baseline ozone change quantified by
 381 the quadratic fit for northern mid-latitudes (Parrish et al., 2020). Symbols color-coded according
 382 to center of time spans of the the reported trends. Error bars indicate the reported 95%
 383 confidence limits of those trends. For clarity, some Cooper et al. (2020) symbols are slightly
 384 offset along the x-axis. (b) Correlation between published ozone trends and center of the time
 385 spans of the trend determinations. Symbols are in the same format as in (a). Solid line indicates
 386 the linear regression with the square of the correlation coefficient annotated, and $t = 0$ reference
 387 indicated by vertical line.

388 **Table 1.** Slopes derived from published trend analyses (with 95% confidence limits) compared
 389 with slopes calculated from the quadratic fit to the northern mid-latitude analysis over the same
 390 time periods. Studies included report results based on mean or median annual or springtime
 391 seasonal data.

| Location | b (slope) (ppb decade ⁻¹) | slope from quadratic fit (ppb decade ⁻¹) | Years of data | Reference |
|---------------------------------|--|--|------------------|-----------------------|
| Mid-troposphere | 1.3 ± 0.9 | 0.1 ± 1.1 | 1994–2016 | Gaudel et al. (2020) |
| Lower troposphere | -0.2 ± 0.9 | 0.1 ± 1.1 | 1994–2016 | “ |
| Centennial, Wyoming | -0.6 ± 0.9 | 0.8 ± 0.9 | 1989–2017 | Cooper et al. (2020) |
| Great Basin NP | 0.5 ± 0.9 | 0.1 ± 1.1 | 1993–2017 | “ |
| Gothic, Colorado | -1.0 ± 0.6 | 0.8 ± 0.9 | 1989–2017 | “ |
| Grand Canyon NP | -0.3 ± 0.7 | 0.8 ± 0.9 | 1989–2017 | “ |
| Centennial, Wyoming | -1.5 ± 1.2 | -0.3 ± 1.2 | 1995–2017 | “ |
| Great Basin NP | 0.2 ± 1.0 | -0.3 ± 1.2 | 1995–2017 | “ |
| Gothic, Colorado | -1.9 ± 0.8 | -0.3 ± 1.2 | 1995–2017 | “ |
| Grand Canyon NP | -1.5 ± 0.8 | -0.3 ± 1.2 | 1995–2017 | “ |
| Centennial, Wyoming | -2.6 ± 1.8 | -1.2 ± 1.4 | 2000–2017 | “ |
| Great Basin NP | -0.5 ± 1.4 | -1.2 ± 1.4 | 2000–2017 | “ |
| Gothic, Colorado | -2.8 ± 1.1 | -1.2 ± 1.4 | 2000–2017 | “ |
| Grand Canyon NP | -2.6 ± 1.1 | -1.2 ± 1.4 | 2000–2017 | “ |
| Great Basin NP ¹ | 2.9 ± 2.3 | 0.4 ± 1.0 | 1994–2014 | Lin et al. (2017) |
| Yellowstone NP ¹ | 2.1 ± 1.9 | 1.8 ± 0.7 | 1988–2012 | “ |
| Pinedale Wyoming ¹ | 0.9 ± 1.8 | 1.5 ± 0.7 | 1990–2012 | “ |
| Mesa Verde NP ¹ | 3.0 ± 1.8 | 0.8 ± 0.9 | 1994–2012 | “ |
| Mid-troposphere ² | 3.1 ± 2.1 | 0.2 ± 1.0 | 1995–2014 | Lin et al. (2015) |
| Mid-troposphere ² | 4.2 ± 1.7 | 2.2 ± 0.6 | 1984–2014 | “ |
| Pacific MBL | 2.7 ± 0.8 | 2.2 ± 0.6 | 1988–2010 | Cooper et al. (2014) |
| Lassen Volcanic NP | 2.7 ± 1.3 | 2.2 ± 0.6 | 1988–2010 | “ |
| Mid-troposphere ² | 4.1 ± 2.7 | 0.8 ± 0.9 | 1995–2011 | Cooper et al. (2012) |
| Mid-troposphere ² | 5.2 ± 2.0 | 2.7 ± 0.6 | 1984–2011 | “ |
| Mid-troposphere ² | 6.3 ± 3.4 | 1.3 ± 0.8 | 1995–2008 | Cooper et al. (2010) |
| Mid-troposphere ² | 7.0 ± 2.2 | 3.3 ± 0.6 | 1984–2008 | “ |
| Pacific MBL | 3.4 ± 0.9 | 2.9 ± 0.5 | 1987–2007 | Parrish et al. (2009) |
| Lassen Volcanic NP ³ | 5.5 ± 2.7 | 3.6 ± 0.6 | 1988–2002 | Jaffe et al. (2003) |

392 ¹ Lin et al. (2017) results are taken from their Figure 13 for stations west of the Front Range of
 393 the Rocky Mountains.

394 ² Results given for 50th percentiles of the springtime seasonal data sets.

395 ³ Jaffe et al. (2003) results are 4 season average from full seasonal data sets in their Table 2.

396 **Table 2.** Parameter values (with 95% confidence limits) derived from quadratic fits for northern
 397 mid-latitudes and for two data sets collected in the western US (Parrish et al., 2020). Intercept
 398 and slope are given for the year 2000.

| Location | a (intercept) ¹ (ppb) | b (slope) (ppb/decade) | c (curvature) (ppb/decade ²) | year _{max} | Years of data |
|------------------------|---------------------------------------|-----------------------------|---|---------------------|------------------|
| Northern mid-latitudes | --- | 2.0 ± 0.6 | -1.8 ± 0.6 | 2005.7 ± 2.5 | 1978–2017 |
| Lassen Volcanic NP | 41.0 ± 0.7 | 2.6 ± 0.7 | -2.4 ± 0.8 | 2005.4 ± 2.2 | 1987–2017 |
| Pacific MBL | 32.9 ± 1.1 | 1.4 ± 1.0 | -2.5 ± 1.1 | 2002.8 ± 2.2 | 1987–2017 |
| derived from trends | --- | 3.4 ± 0.9 | -2.9 ± 0.8 | 2005.8 ± 2.2 | 1984–2017 |

399 ¹ A value for a is not returned for the fit to the normalized monthly means and the linear fit to
 400 the published trends.

Geophysical Research Letters

Supporting Information for

Long-term Baseline Ozone Changes in the Western US: A Synthesis of Analyses

David D. Parrish^{1,2}, R. G. Derwent³, I. C. Faloona^{2,4}

¹David D. Parrish, LLC, Boulder, CO, 80309 USA

²Air Quality Research Center, University of California, Davis, CA, 95616 USA

³rdscientific, Newbury, Berkshire, UK

⁴Department of Land, Air, & Water Resources, University of California, Davis, CA, 95616 USA

Contents of this file

Text S1 to S6
Figures S1 to S3

Introduction

This supporting information presents additional discussion of the northern mid-latitude ozone distribution with illustrative figures and their explanations, which support the analysis and interpretation of results in the main text. Figure S1 is an estimation of the important time scales influencing ozone concentrations in the northern mid-latitude troposphere and their dependence on altitude. Figure S2 is a plot derived from the multi-model ensemble of troposphere ozone budgets compiled in Table 5 from Stevenson et al. (2006). Figure S3 illustrates the autocorrelation functions from two de-seasonalized ozone time series used in this work (Pacific MBL and Lassen NP.)

Text S1. Vertical Dependence of Major Tropospheric O₃ Timescales

In order to compare relevant time scales of vertical convective mixing, horizontal advection, dry deposition, and photochemical destruction as a function of height we estimated them in the following manner and present them in Figure S1. We use the NCEP Reanalysis Seasonal Climate composites page (<https://psl.noaa.gov/cgi-bin/data/composites/printpage.pl>) to derive annual mean values of air temperature, specific humidity, and zonal wind speeds from 30°N to 60°N at each of eight altitudes from 1–8 km to establish mean conditions for chemical reaction rates and horizontal advection rates. To estimate the vertical mixing due to convection we use the ERA-40 reanalysis data of convective mass flux as reported in Doherty et al. (2005) for the zonal band from 30-60N. The mass fluxes are converted to vertical velocities by the air density and these are added in series to get the progressive time scales for mixing up/down into the free troposphere. To derive time scales for dry deposition we link these convective rates with an average deposition velocity of 2.1 mm/s with the understanding that at midlatitudes in the Northern Hemisphere the surface is about half ocean ($v_d \sim 0.25$ mm/s) and half land ($v_d \sim 4.0$ mm/s). The photolysis frequencies for generating excited atomic oxygen, O(¹D), as a function of height are taken from observations over the North Pacific presented in Hall et al. (2018) from the ATom-1 mission and scaled for diurnal and annual averaging. Reaction rates for OH + O₃ and HO₂ + O₃ and O(¹D) + H₂O, N₂, and O₂ are calculated from the coefficients provided in the JPL publication 15-10 (Burkholder et al., 2015). Representative daytime/spring tropospheric profiles of OH and HO₂ were estimated based on Tan et al. (2001).

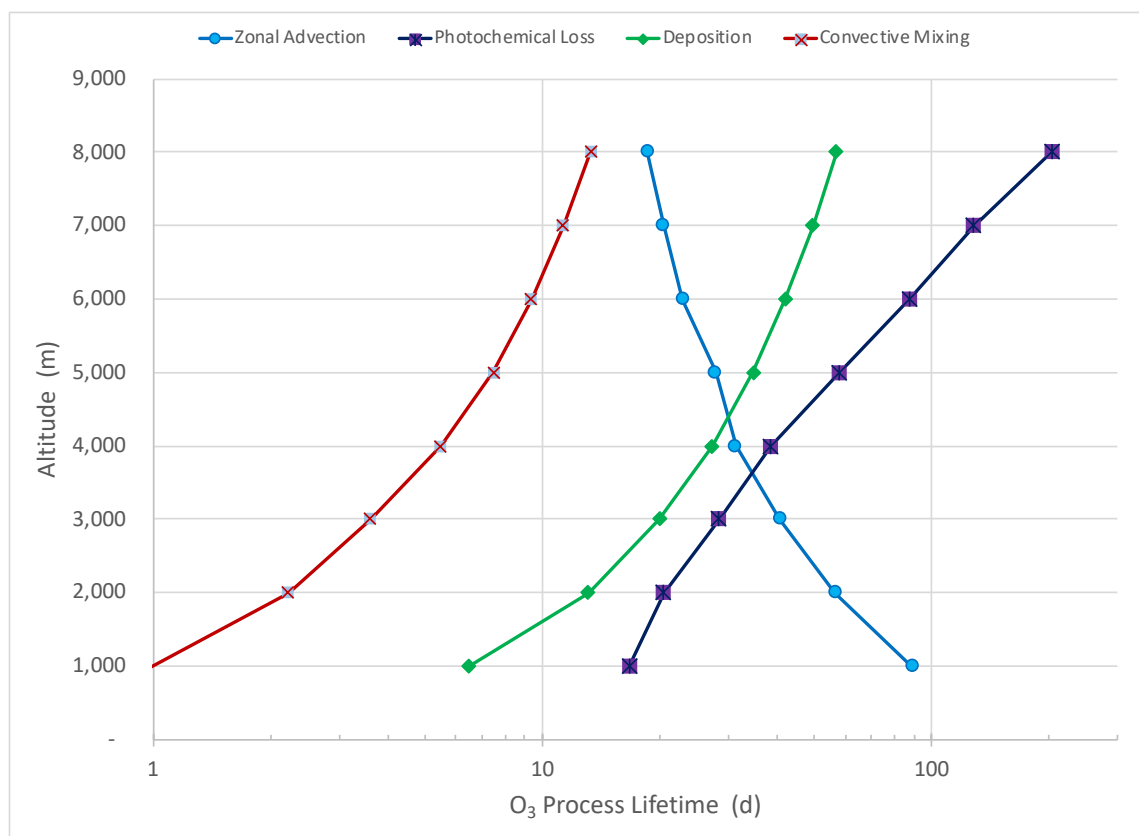


Figure S1: Vertical Dependence of Major Tropospheric O₃ Timescales in the Zonal Band from 30°N – 60°N.

Text S2. Correlation Among 26 Global Chemical Transport Models' Gross Production and Loss of Tropospheric Ozone

A common relationship found in global chemical transport models with respect to the tropospheric ozone budget is that the gross photochemical loss rates are typically about 5-10% smaller than the gross production rates, regardless of their absolute magnitude. Figure S2 plots the 21 loss and production values from the models surveyed in Stevenson et al. (2006), and also includes the background tropospheric run of Crutzen et al. (1999). Aside from the difference in absolute values in all the models spanning about a factor of two, the production and loss terms tend to compensate to a great degree due to the related photochemical cycles of O_3 , HO_x , RO_2 , and NO_x . The one counter-example is the run without anthropogenic sources reported by Crutzen et al. (1999) where the high loss rate is sustained by an extremely large stratospheric source in that model, which was two and a half times larger than the model mean in Stevenson et al. (2006).

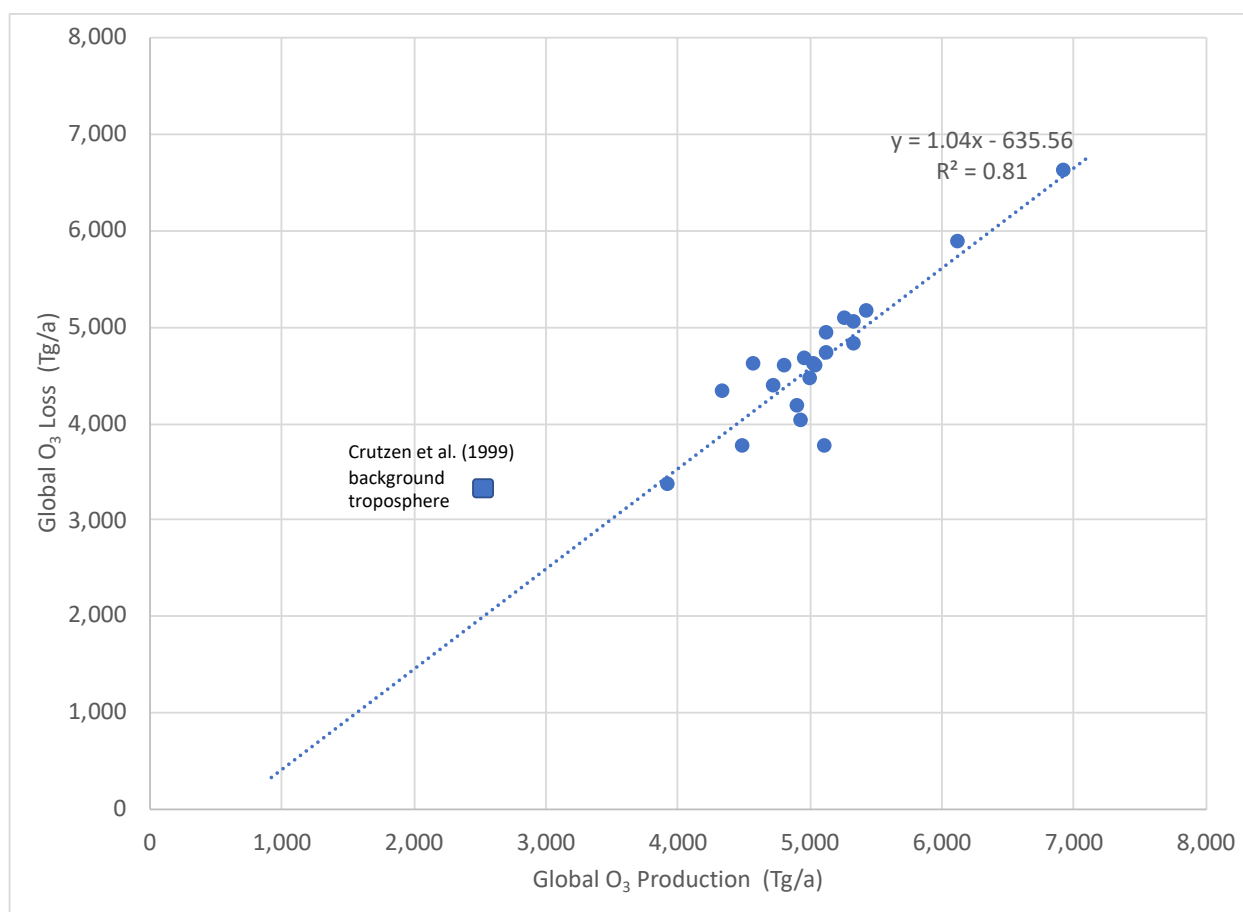


Figure S2: Correlation of gross photochemical production and loss rates among 21 chemical transport models tabulated in Stevenson et al. (2006).

Text S3. Similarity of zonal mean ozone at northern mid latitudes

The conceptual picture for understanding the long-term changes of ozone at northern mid-latitudes recognizes that the circum-global transport time is significantly shorter than the net lifetime of ozone, which implies that a relatively constant zonal mean ozone concentration exists. The circum-global transport time is about 25 to 30 days, as indicated by a simple tracer experiment of a surface release using a global Lagrangian chemistry-transport model (STOCHEM-CRI; Derwent et al., 2018) driven by 1998 meteorological fields from the UK Meteorological Office Unified Model archive (Collins et al., 1997). The STOCHEM-CRI model finds that the northern mid-latitude ozone lifetime is about 50 to 60 days, when only loss processes are considered. However, in situ ozone production from photochemical oxidation of precursor compounds proceeds simultaneously with the photochemical and dry deposition loss processes to partially balance the loss; consequently the mean net lifetime of ozone in an isolated air parcel at northern mid-latitudes is several months or longer. Meridional eddy fluxes of ozone can lead to perturbations of local concentrations, but on average the meridional gradients of ozone are small at 30 and 60 N (e.g., Figure 2 of Crutzen et al., 1999), as are the mean meridional winds (e.g., Figure 7.17 of Peixoto & Oort, 1992); thus meridional advection does not, on average, significantly affect the mid-latitude budget of tropospheric ozone.

Within the midlatitude troposphere the rate of photochemical ozone loss decreases, while the speed of advection increases with altitude. Writ large, vertical gradients in baseline ozone arise due to the elevated source in the stratosphere coupled to the surface sink of dry deposition. Modeling of background ozone by Crutzen et al. (1999) indicates that net photochemical production above about 800 hPa in the northern midlatitudes ranges from -1.0 ppb/day in the lower troposphere to +0.2 ppb/day in the upper troposphere, further reinforcing the overall positive vertical gradient in baseline ozone, and suggesting a lifetime of ~100 days with respect to net photochemistry throughout the bulk of the troposphere. However, typical convective mass flux schemes suggest that the overturning time scale is less than ~ 20 days at northern mid-latitudes (Figure S1), which tends to minimize the vertical ozone gradient (e.g., Fig 1B, Lelieveld & Crutzen, 1994). Overall, the long net ozone lifetime, zonal transport, and relatively rapid vertical overturning implies that a mean ozone concentration is established on a time scale of weeks to months, and that this mean concentration must be similar throughout northern mid-latitudes. This picture also implies a relatively smooth and systematic seasonal cycle of ozone in baseline air masses.

Text S4. Ozone variability at northern mid latitudes

Ozone varies about the zonally similar mean ozone concentration on a wide spectrum of shorter and longer time scales. The mean ozone concentration varies seasonally, due to seasonal changes in sources and sinks. An air parcel within the circulating river of air receives sporadic injections of ozone and its photochemical precursors from European, Asian and North American anthropogenic sources and from the natural stratospheric source. Ozone injected from the extremely arid stratosphere maintains an anti-correlation with water vapor across vast expanses of the troposphere (Newell et al., 1999) extending its photochemical lifetime with respect to OH production. The infusions of anthropogenic NO_x and VOC precursors into the general tropospheric flow, accelerate photochemical ozone production, but also concomitantly enhance photochemical losses as well due to increases in HO_x abundance and production of NO₃ radicals in the dark. Consequently, significant deviations from the circulating mean ozone are brought about in the environment of prolonged net photochemical lifetimes. In addition, air parcels with different ozone production and loss histories are entrained from and exported to

higher and lower latitudes. The overall result is local and regional, quasi-chaotic ozone variability superimposed on the mean concentration.

Text S5. Quadratic fits vs. Linear trend analysis

Cooper et al. (2020) discuss two particular problems with the use of polynomial fits to characterize long-term ozone changes. The first is the inability of polynomials to describe multi-year ozone fluctuations that can be fit by other techniques. For our purposes, this inability is an advantage rather than a problem, because we aim to avoid the influence of multi-year ozone fluctuations, i.e., interannual variability, which obscure the systematic decadal scale changes that are our focus. The second identified problem is that the long-term change determination over the entire time span of the measurements, including at the beginning of the data record, is impacted by additional data added to the end of a time series as new measurements are made. The results of polynomial fits do change in this manner, because the parameter values are more precisely determined by longer time series, but these more precise parameter values generally fall within the confidence limits of the earlier derived, less precise parameters. Moreover, fits to progressively longer time series allow for the inclusion of additional terms in the polynomial fits, allowing flexibility in fitting the later data, and minimizing changes of the fit to the earliest measurements. Notably, this second problem also characterizes linear trend analysis, as the derived trend generally changes as a time series of measurements is extended; however linear trend analysis does not provide a means for the functional form to evolve as non-linear changes become apparent. Parrish et al. (2019) show that the polynomial fits, as used in this work, provide an effective approach for quantifying non-linear, long-term changes of atmospheric concentrations. The ability of polynomial fits to effectively quantify non-linear, long-term changes in the presence of substantial interannual variability is more important for our purposes, than are any problems.

Text S6. Autocorrelation functions for two of the time series used in this analysis (Pacific MBL and Lassen Volcanic NP)

The de-seasonalized monthly ozone residuals for two of the time series in the analysis of Parrish et al. (2020) are used to calculate their autocorrelation functions shown in Figures S3. The decorrelation times indicated in the annotations are used to correct the confidence limits of uncertainties of the parameters derived in the long-term change fits. While the majority of the autocorrelation fades after 1-2 months, lingering autocorrelation out to 3 years can be seen in the Pacific MBL data, and from 2-4 years in the Lassen NP data. Failure to adequately account for autocorrelation of data over the full spectrum of significant time scales results in an overestimation of the accuracy of parameter values (i.e., underestimations of their confidence limits) derived from any linear or non-linear regression analyses such as the literature results discussed in our manuscript and included in Table 1. This lingering autocorrelation issue is at least partially overcome by the 2 year means used in deriving the Figure 1.

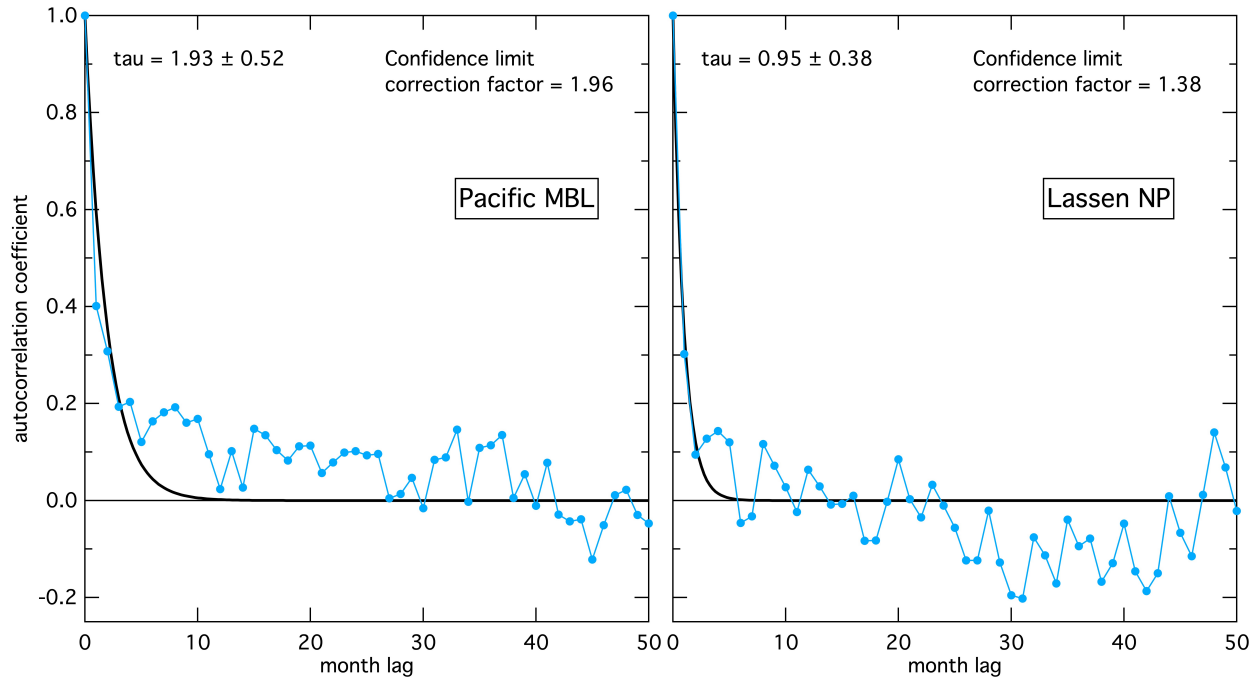


Figure S3: Autocorrelation functions for the (left) the 21 year time series in the Pacific MBL and (right) the 15 year time series from Lassen Volcanic NP. An exponential function is fit to the near-term function to estimate the correction to confidence limits of the decadal trends reported in the literature.

Additional References:

- Burkholder, J. B., Sander, S. P., Abbatt, J. P. D., Barker, J. R., Cappa, C., Crouse, J. D., Dibble T. S., et al. (2015). *Chemical kinetics and photochemical data for use in atmospheric studies; evaluation number 18*. Pasadena, CA: Jet Propulsion Laboratory, National Aeronautics and Space Administration.
- Collins, W. J., Stevenson, D. S., Johnson, C. E., & Derwent, R. G. (1997). Tropospheric ozone in a global-scale three-dimensional Lagrangian model and its response to NO_x emission controls, *Journal of Atmospheric Chemistry*, *26*, 223-274.
- Crutzen, P. J., Lawrence, M. G. & Pöschl, U. (1999) On the background photochemistry of tropospheric ozone, *Tellus B: Chemical and Physical Meteorology*, *51*:1, 123-146, DOI: 10.3402/tellusb.v51i1.16264
- Derwent R. G., Parrish D. D., Galbally, I. E., Stevenson, D. S., Doherty R. M., Naik, V., & Young, P. J. (2018). Uncertainties in models of tropospheric ozone based on Monte Carlo analysis: Tropospheric ozone burdens, atmospheric lifetimes and surface distributions, *Atmos. Environ.* *180*, 93–102, doi.org/10.1016/j.atmosenv.2018.02.047
- Doherty, R. M., Stevenson, D. S., Collins, W. J., & Sanderson, M. G. (2005). Influence of convective transport on tropospheric ozone and its precursors in a chemistry-climate model, *Atmos. Chem. Phys.*, *5*, 3205–3218, <https://doi.org/10.5194/acp-5-3205-2005>.
- Hall, S. R., Ullmann, K., Prather, M. J., Flynn, C. M., Murray, L. T., Fiore, A. M., Correa, G., Strode, S. A., Steenrod, S. D., Lamarque, J.-F., Guth, J., Josse, B., Flemming, J., Huijnen, V., Abraham, N. L., & Archibald, A. T. (2018). Cloud impacts on photochemistry: building a climatology of photolysis rates from the Atmospheric Tomography mission, *Atmos. Chem. Phys.*, *18*, 16809–16828, <https://doi.org/10.5194/acp-18-16809-2018>.
- Lelieveld, J., & Crutzen, P. J. (1994). Role of deep cloud convection in the ozone budget of the troposphere, *Science*, *264* (5166) 1759-1761
- Newell, R. E., Thouret, V., Cho, J. Y. N., Stoller, p., Marengo, A., & Smit, H. G. (1999). Ubiquity of quasi-horizontal layers in the troposphere, *Nature*, *398*(6725) 316-319.
- Peixoto, J. P., & Oort, A. H. (1992). *Physics of Climate*. New York, NY: American Inst. of Physics.
- Stevenson, D. S., et al. (2006), Multimodel ensemble simulations of present-day and near-future tropospheric ozone, *J. Geophys. Res.*, *111*, D08301, doi:10.1029/2005JD006338.
- Tan, D., I. Faloon, J.B. Simpas, W. H. Brune, et al. (2001). OH and HO₂ in the tropical pacific: Results from PEM-Tropics B. *J. Geophys. Res.*, *106* (D23):32,667-32,681.